CANADIAN JOURNAL OF EXPLORATION GEOPHYSICS
VOL. 30, NO. 1 (JUNE 1994), P. 28-38

# HIGH-RESOLUTION SEISMIC REFLECTION SURVEYS TO DETECT FRACTURE ZONES AT THE AECL UNDERGROUND RESEARCH LABORATORY

D.J. GENDZWILL[1], M.H. SERZU[2] AND G.S. LODHA[2]

## ABSTRACT

A high-resolution seismic reflection experiment was conducted on the 240-m level at the Underground Research Laboratory of AECL in February 1992 to test whether the method could detect fracture zones in the granite. High-resolution seismic methods were considered desirable because of the size and depth of the target.

Data were collected using a hammer as the seismic source. The geophones were bolted to the granite rock. Several noise patterns, not common in surface seismic data, had to be suppressed before reflections could be seen. After computer processing of the data, well-defined seismic compressional wave reflections with a dominant frequency near 1200 Hz were detected. Fracture Zone 2 (FZ-2), which is 50 m below the 240 level, was detected as a narrow band of parallel reflectors. Shear wave reflections from FZ-2 were also identified. Several other thin fracture zones were detected but some reflectors at depths of 180 m or more from the survey line were not uniquely identified. Some of the reflections were confirmed with a synthetic seismogram. Reflectivity of the zones is due to changes in acoustic impedance of the altered and broken granite rock. A repeat of the survey using blasting caps as the seismic source produced similar results. A comparison with ground probing radar data from the shallow part of FZ-2 in room 207 showed that radar and seismic reflections originated from different sections of the same fracture zone.

## INTRODUCTION

The Underground Research Laboratory (URL) of Atomic Energy of Canada Ltd. (AECL) is located in the granitic Lac du Bonnet Batholith near Pinawa, Manitoba (Figure 1). The URL has a vertical shaft and main working levels at depths of 240 m and 420 m. It is operated for geoscience and geotechnical research under the Canadian Nuclear Fuel Waste Management Program. One of the research objectives is the detection, evaluation and characterization of fractures in granitic rock. This study presents the results of a test of the seismic reflection method to detect fractures by surveys conducted within the underground openings of the URL.

Figure 1 shows a location map and general geology of the URL in plan and in vertical section. At surface, there is a pink, mostly porphyritic, granite containing several sets of pervasive subvertical fractures including both tensile and compressive types (Brown et al., 1989). Below the pink granite is a grey granite, commonly homogeneous, equigranular and not fractured. Bands of gneissic granite and xenolithic granite are horizontal to gently dipping and form a broad antiform structure (Brown et al., 1989) which dips to the southeast near the URL. Xenolith bands contain more than 25% xenoliths composed of tonalite, amphibolite and other wall rocks, altered in some places to biotite rich granite.

Two low-dipping fracture zones, called Fracture Zone 3 (FZ-3) and Fracture Zone 2 (FZ-2), were intersected by the shaft at the URL where they are about 23 m and 13 m thick, respectively. These are reverse faults which show displacements up to about 8 m (Brown et al., 1989). They dip southeasterly at the URL and tend to be subparallel to the gneissic banding and xenolithic layers. These fracture zones contain regions of high permeability and they control the movement of groundwater through the rock. FZ-3 is contained within the pink granite. FZ-2 (Figures 1 and 2), the object of the seismic survey, is within the grey granite below the 240 level, except for the FZ-2.5 which intersects the shaft above the 240 level and forms the boundary between grey and pink granite. Other splays exist below FZ-2 (FZ-1.9, FZ-1.8, etc.). Regional stress fields are markedly different in the pink and grey granite above and below FZ-2 (Martin, 1990) and the subvertical fractures are only found above FZ-2.

Fractured rock tends to absorb seismic energy through various loss mechanisms and to reduce the velocity of seismic waves. Fractured rock is less stiff in its elastic properties than unfractured rock, resulting in reduction of seismic velocity. A good seismic reflection from a zone of intense fracturing such as FZ-2 will occur provided that the zone is thick enough and smooth enough to provide a specular

Manuscript received by the Editor May 11, 1994; revised manuscript received September 20, 1994; manuscript accepted September 22, 1994.
[1]Department of Geological Sciences, University of Saskatchewan, Saskatoon, Saskatchewan S7N 0W0
[2]Applied Geoscience Branch, AECL Research, Whiteshell Laboratories, Pinawa, Manitoba R0E 1L0
Support for this project came from an operating grant provided by the Canadian Nuclear Fuel Waste Management Program which is jointly funded by AECL and Ontario Hydro under the auspices of the CANDU Owners Group (COG). Potash Corporation of Saskatchewan loaned the use of their Bison 9000 seismograph. Data processing was done at the University of Saskatchewan Geophysical Computing Centre. Field work was ably assisted by Cao Lu and Doug Neilson, graduate students at the University of Saskatchewan. Doug Neilson also assisted with drafting of figures. Critical review of this manuscript by N. Soonawala, C.C. Davison, S.H. Whitaker and anonymous journal reviewers has been valuable.

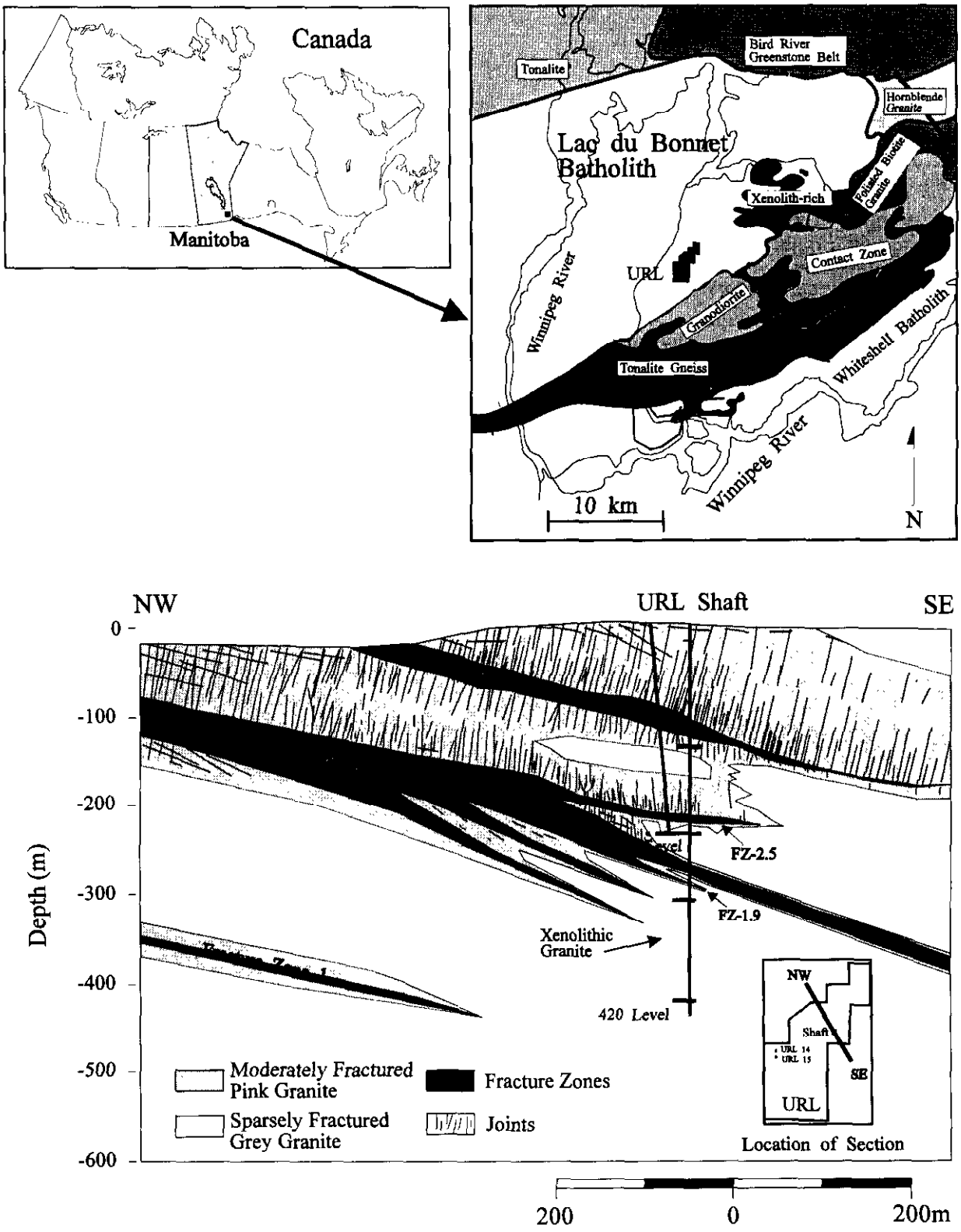


**Fig. 1.** Upper left: location of the URL. Upper right: regional geology. Lower: NW-SE geological cross-section at the URL (modified after Brown et al., 1989).

reflecting surface for the dominant seismic wavelength. A sonic log was available for borehole URL-6 (Figure 2), which penetrated the rock near the URL shaft, and a synthetic seismogram was calculated from it (Figure 3).

Previous seismic tests at URL have included vertical reflection surveys from surface, cross-hole tomography surveys, passive monitoring of microseismic emissions and borehole acoustic logging. Most recently, Kim et al. (1994)

have described results of surface seismic reflection surveys. However, the seismic reflection profiling technique had not been previously tested underground. Successful application in Saskatchewan potash mines (Gendzwill and Brehm, 1993) suggested that the method might be useful at URL. Therefore, in January 1992 the underground reflection method was tested from the 240 level to detect FZ-2, about 50 m below the 240 level (Figure 2).

Conditions inside the URL are different from conditions for seismic surveys at the surface. In the URL, the rock of the roof, walls and floor is hard granite. There is no weathering layer to absorb high frequencies. In our tests we found dominant reflection frequencies near 1200 Hz, more than ten times the frequency content of "normal" surface seismic data. The compressional wave velocity of the unfractured granite at this depth is fairly constant at 5800 m/s and at 1200 Hz the wavelength is about 5 m. The shear wave velocity is 3350 m/s but the frequency is somewhat lower so the wavelength is still about 5 m. Such high frequencies should detect fracture zones down to about 1 m in thickness.

In an underground environment, seismic reflections may be created by any surface below, above, or to the side of the recording line. However, seismic energy is directed by the tunnel opening which acts as a ground plane, especially if the seismic wavelength is smaller than the opening. A source position on the floor of the opening favours production of downgoing waves and receivers on the floor respond best to upgoing reflections. Reflections from above the roof must travel around the opening to excite geophones placed on the floor, hence, reflections from above are strongly attenuated. Nevertheless, geometric effects and out-of-plane reflections are still a problem as in any three-dimensional seismic investigation. In this survey, geometric problems were mitigated to some extent by the fact that the seismic line was almost parallel to the strike of the target fracture zone, ensuring that reflections were normal to the fracture surface.

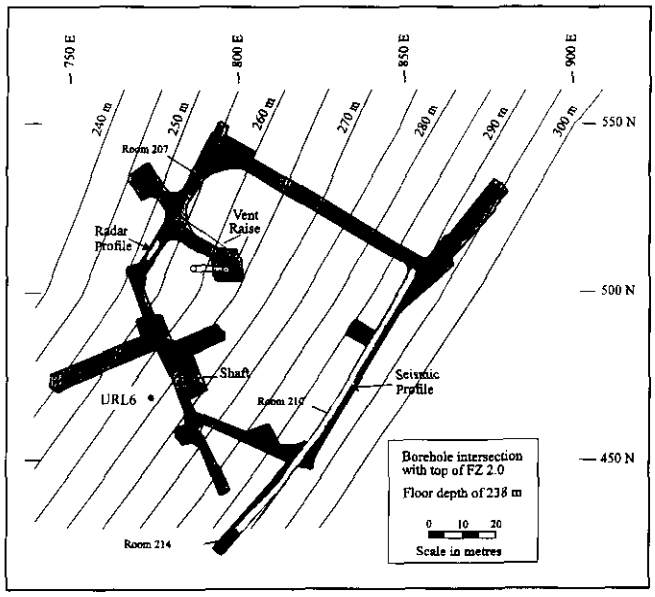


**Fig. 2.** Plan of 240 level URL with structure contours of top of Fracture Zone 2 superimposed (Everitt and Reed, 1989). Locations of the seismic profile in rooms 214 and 210, the radar profile in room 207 (Holloway, 1992) and borehole URL6 are also shown.

## Method

### Field procedure

In high-resolution seismic reflection surveys, it is important to record the signal with adequate spatial and temporal sampling to avoid aliasing problems.

The recording equipment was a Bison Instruments Model 9000, 24-channel stacking seismograph. Data were recorded using a 0.2 ms sample rate, a filter pass from 128 Hz to 2000 Hz, the floating point gain set to medium, and a 200-ms record length. However, only 80 ms of the record was used because air noise increased after 80 ms.

Mark Products L25E, 50-Hz single geophones were used, spaced 1 m apart, in a line 83 m long. A 48-channel roll-along switch and cables allowed a convenient CMP shooting geometry.

Geophones must be coupled firmly to the rock to detect frequencies around 1000 Hz. Small steel brackets (10 x 2.5 x 0.6 cm) were fastened to the rock with a Hilti bolt. Each bracket had a threaded hole near one end for the geophone, a hole in the centre for the bolt, and a bend in the middle so that it contacted the rock solidly at three points (Figure 4). Nevertheless, resonance of the geophone, bracket, and rock coupling were a source of high-frequency noise which was reduced with predictive deconvolution.

At the time of the survey the floor of the 240 level was concrete paved except for a narrow drainage ditch along one wall. Geophones were bolted to the rock in the drainage ditch but at one intersection, 8 m wide, there was no drainage ditch so geophones were bolted to the concrete. Data collected with hammer points or geophones on concrete proved to be of such poor quality that they could not be used, reducing the CMP fold in those areas.

The energy source was a 4.5 kg sledgehammer with an inertia switch on the handle to trigger the seismograph. The inertia switch introduced a 2.5-ms delay in the recorder start time. No striking plate was needed on the hard rock surface. Hammer arrays were used, striking the floor at 5 points separated by 0.5 m, for a total length of 2 m, stacking all blows into a single record on the Bison. Array centres were moved 1 m for successive records. The minimum offset was 15 m to avoid unwanted hammer noise travelling through the air, the maximum offset was 38 m. Single-ended geometry was used, hammering at both ends of each geophone spread to achieve 24-fold coverage with the 24 channels. Figure 5 shows the array response for the hammer array, stack array (Anstey, 1986) and combination. Source-generated surface waves at the underground mine opening propagate with a speed of 3350 m/s (*S*-wave velocity in granite). As a result, the frequency of surface waves along the floor of the underground mine is higher than those of corresponding waves generated at the surface. The hammer array and stack array design tend to attenuate these high-frequency surface waves (> 190 Hz).

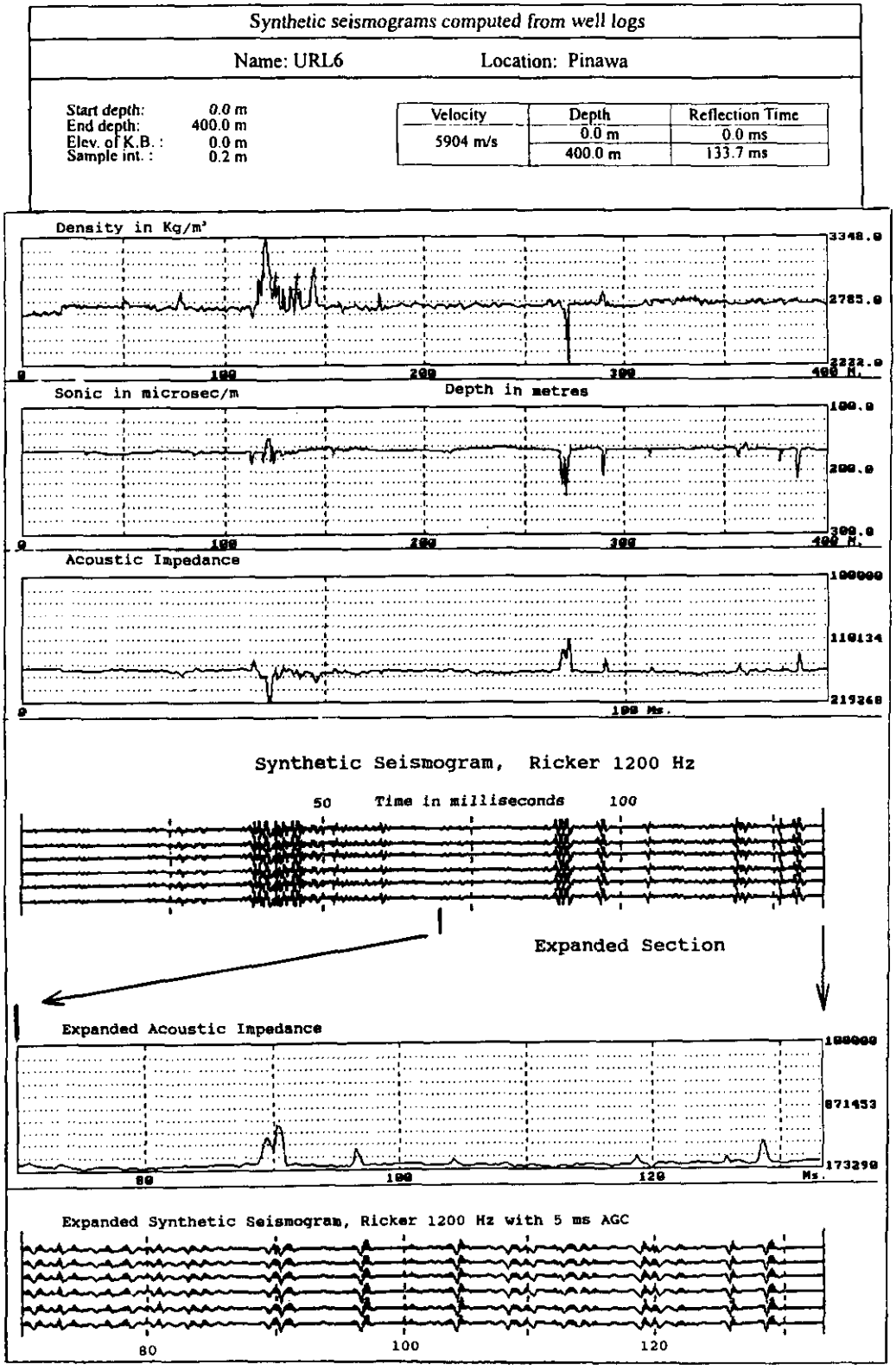


**Fig. 3.** Synthetic seismogram from sonic and density logs for borehole URL-6 with 1200-Hz Ricker wavelet, matching the field seismogram. Expanded section from 70 ms (240-m depth) corresponds with the underground seismic zone of investigation. The expanded section synthetic seismogram has been filtered with 5 ms AGC operator, similar to the field seismogram.

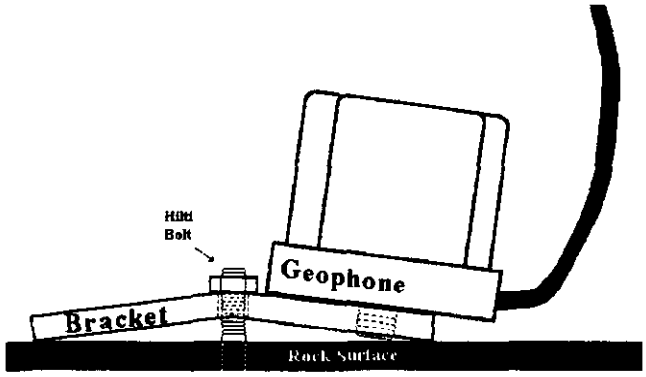


**Fig. 4.** Sketch of geophone and holder.

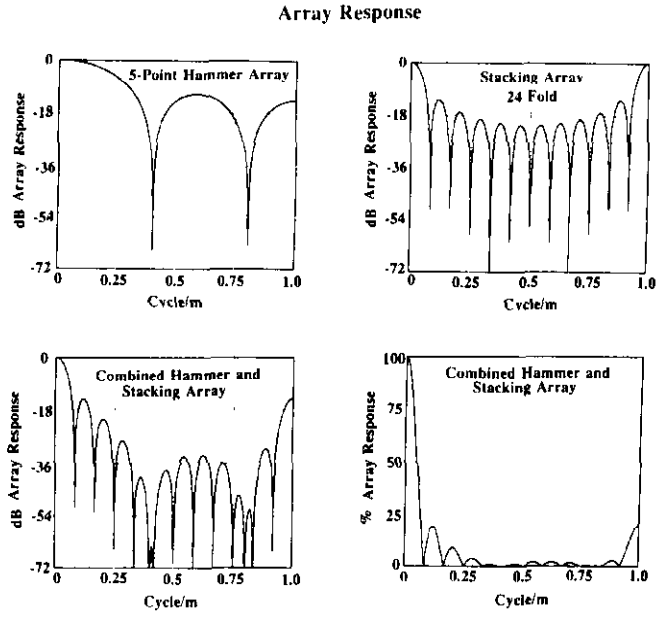


**Fig. 5.** Array response of hammer and stack arrays.

A portion of the line was repeated, using detonating caps as the energy source, in order to verify the reproducibility of data. Caps were fired singly in 25-cm deep holes separated by 1 m. A 15-m offset was also used for the cap profile but only 12-fold coverage was achieved because shots were fired at only one end of each geophone spread.

## Computer processing

Processing of the high-frequency data was done with VISTA, a commercial processing package that runs on a desk-top computer.

The original records are very noisy with no recognizable reflections. The spectra show energy peaks between 600 Hz and 1500 Hz for different geophones but most of this is noise, related to coupling conditions between the geophone, steel bracket and rock.

Automatic Gain Control (AGC) was used instead of programmed gain recovery because AGC seemed to produce more uniform amplitudes in the noisy data. After AGC, the resonant oscillations are more continuous, sharpening the spectral peaks, but reflections are still not apparent. The AGC window of 5 ms was selected by trial, matching the anomaly structure in the seismogram.

Predictive deconvolution was used to reduce resonance in the records. A 5-ms length and 0.4-ms lag was used for the predictive deconvolution filter. This was chosen by trial, using autocorrelation as a guide, to improve the visual quality of reflections. In this display, some reflections can be seen. Fifty-one percent of the average input AGC signal amplitude is removed by deconvolution. The removed energy consists of the resonant vibrations of the geophones. The Fourier spectra show a relatively uniform amplitude over a broad frequency range, the so-called whitening effect.

Some of the noise is due to multiple surface waves, reflected from both ends of the tunnel opening and travelling in both directions at 3350 m/s, the shear wave velocity for granite. An *f-k* filter was used to attenuate noise travelling slower than 3600 m/s. Reflections are clearly seen after the *f-k* filter. After both deconvolution and *f-k* filtering, the average signal amplitude is reduced to about 25% of its starting value. Fourier spectra show the remaining energy to be mostly in the range of 400 Hz to 1750 Hz. Figure 6 shows a hammer record, the same record after AGC, after predictive deconvolution, and after *f-k* filtering. Figure 7 shows the corresponding Fourier amplitude spectra. Only 30 ms of data are displayed for clarity.

Elevations along the profile vary less than 0.5 m and there is no low-velocity weathering layer so elevation corrections are small. Surface-consistent automatic static corrections were calculated separately for the *P*-wave and the *S*-wave stacks.

Velocity was picked from the first arrivals on the records. The compressional wave velocity is 5800 m/s and the shear wave velocity is 3350 m/s. Semblance analyses of stacking velocity on common-midpoint gathers show that the *P*- and *S*-wave velocities for the whole record are the same as from first-break analyses.

Stacked sections were made with both *P*- (Figure 8) and *S*- (Figure 9) wave velocity. The difference in moveout permits a distinction of wave type in the early part of the records. After about 40 ms there is not enough moveout to permit clear distinction between *P*- and *S*-waves so the same events appear on both stacks.

Similar processing procedures were applied to the data collected with electric blasting caps. Results are shown in Figure 10. Comparison of the hammer and cap data sets shows that the main reflection events appear on both stacked record sections, giving some confidence in the validity of the reflections.

## Results

### Compressional wave stack

The compressional wave stack of the hammer profile is shown in Figure 8. Data quality appears better in the northeast half of the section than in the southwest portion due to

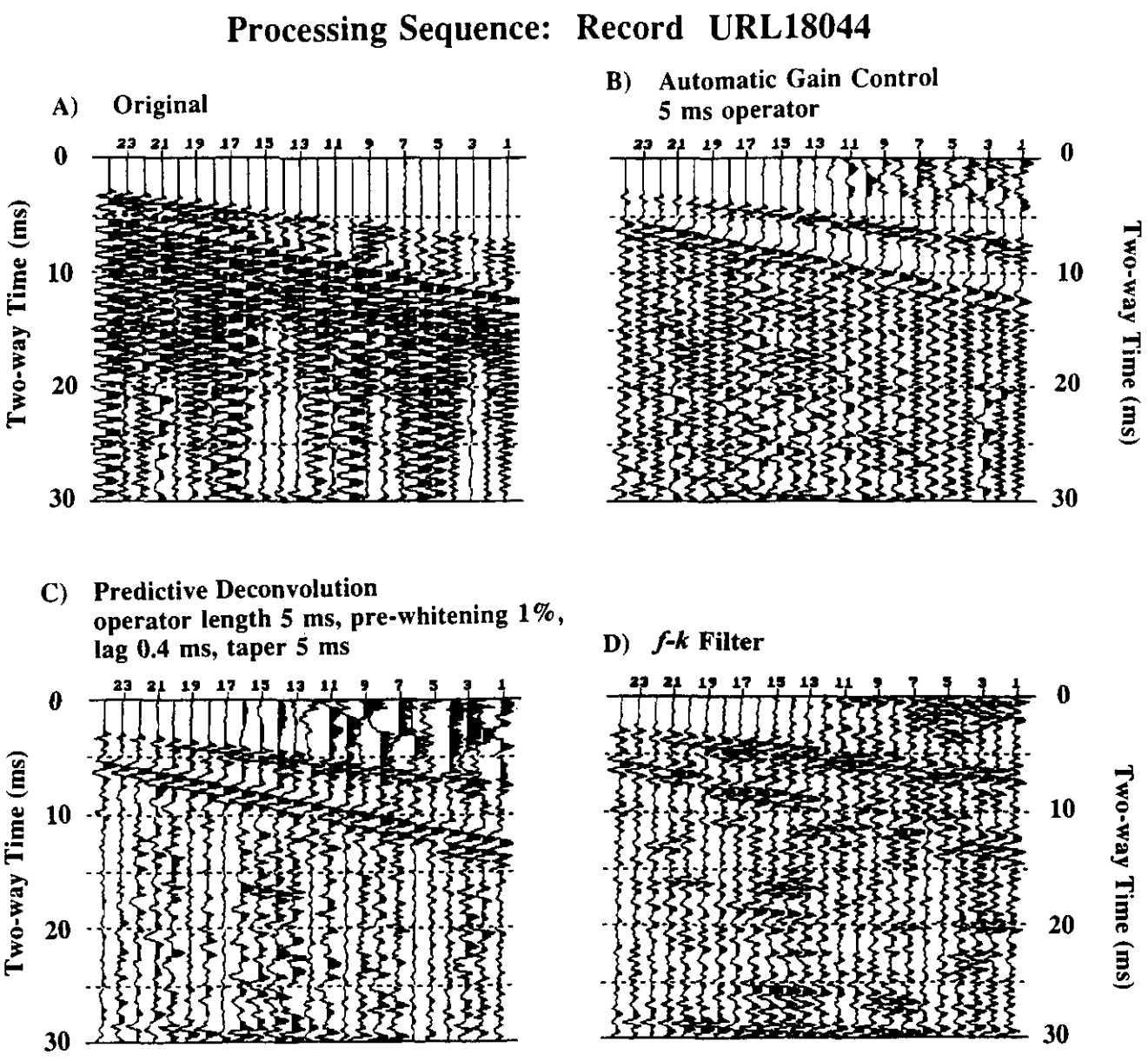


**Fig. 6.** Example of processing sequence on record 18044.

poor coupling of the geophones on the cement floor in the southwest. Reflections are portrayed with no correction for dip or out-of-plane geometry. There is no cross-line data to allow a dip correction. The profile is nearly parallel to the strike of FZ-2 (Figure 2) so the indicated depths may be close to the true normal distance from 240 level.

The first clear reflection occurs at 15.5 ms in the northeast half of the profile, corresponding to the top of FZ-2. The depth to the top of the fracture zone should be 52 m under room 210 as shown on Figure 2, so the reflection time (at 5800 m/s) should be 18 ms, more than the observed time. The difference can be explained by a delay in the recording start time. There is a small delay between the instant of impact of the hammer and the closure of the inertia switch mounted on the handle, so the start time is delayed, causing an apparent early arrival of reflections. Depths shown on the figures include a correction for the start-time delay.

FZ-2 appears as a narrow band of reflectivity between about 15.5 ms and 19.5 ms, corresponding to a thickness of 11.6 m, the expected thickness in this area. The top and bottom of FZ-2 are represented and a reflection also appears inside the zone, possibly marking a change in the intensity of fracturing.

A single reflection appears around 22 ms identifiable over most of the line, which may be correlated to the splay FZ-1.9, below FZ-2. Another reflection, at about 28 ms in the northeast end of the line is not clearly identifiable in the southwest. It may be correlated to the splay FZ-1.8.

The detailed section of the synthetic seismogram (Figure 3) shows reflections similar to those on the reflection seismogram. A direct comparison with the field data is shown on Figure 11 where the synthetic reflections correlate well with field reflections from the top and bottom of FZ-2, and possibly

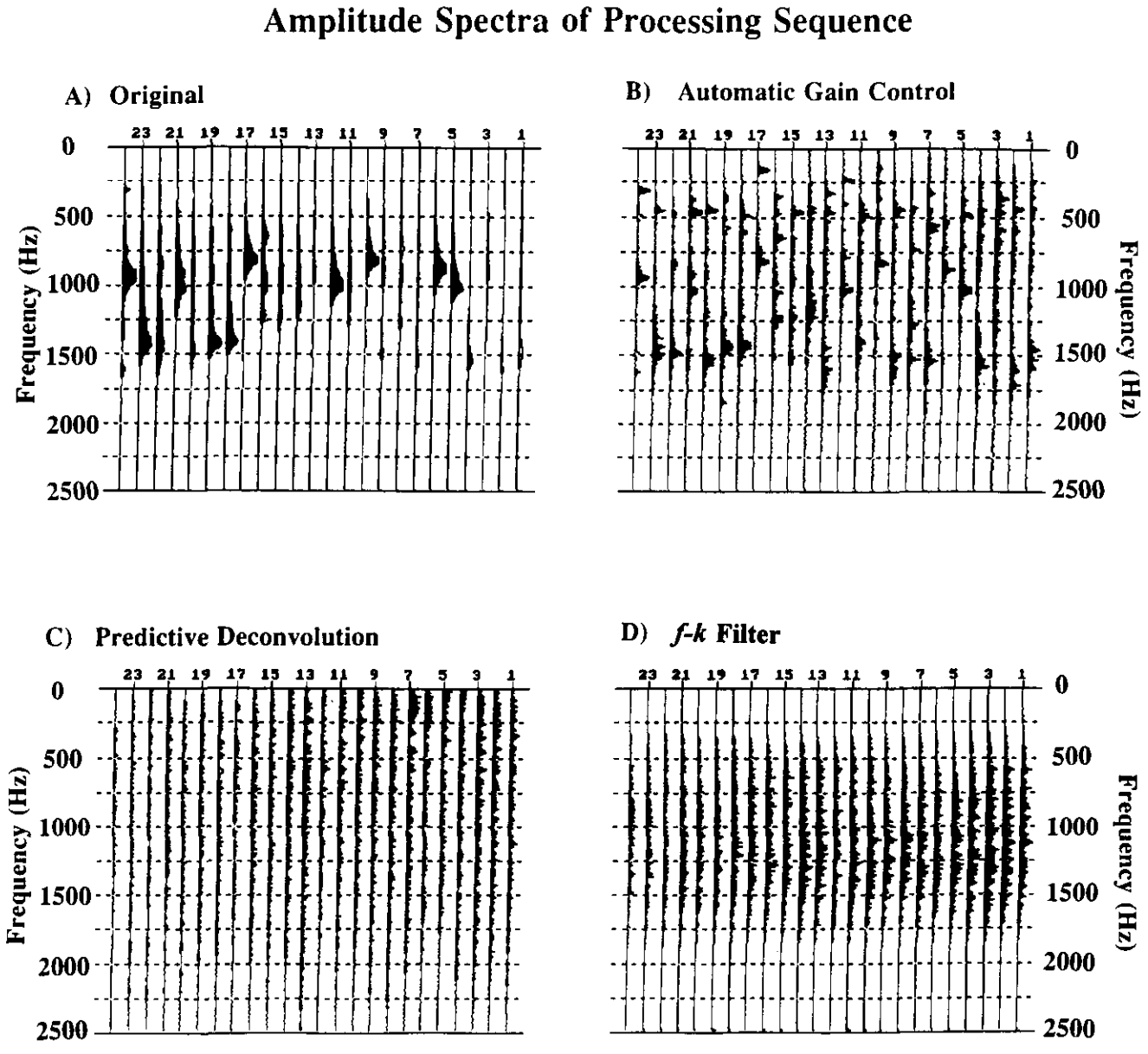


**Fig. 7.** Example Fourier spectra of records shown in Figure 6.

with FZ-1.8 and FZ-1.9. URL6 does not coincide with the seismic line but it is close enough (Figure 2) to have some confidence in these correlations.

Several good reflections occur between 60 ms and 70 ms but their source can not be identified clearly. There are no known fracture zones in these positions to cause the reflections but there are several other possible causes. A xenolithic granite exists at about the right depth but it is not clear if it has sufficient velocity or density contrast to cause a reflection. An inclined tunnel at the 420 level is at the right depth to account for the reflection time but it is not clear how a smooth, continuous reflection would be generated by a narrow tunnel. The reflections may be from an unknown steeply dipping feature out of the plane of the survey. The strike would have to be almost parallel to room 210. The location of this reflector can not be uniquely interpreted using data from only one seismic line.

A dipping feature exists between 25 ms and 40 ms. The curved pattern suggests that it could be a diffraction. The apex of the curve is at about 30 m chainage, directly opposite the shaft which is about 42 m away (Figure 2). Therefore, the

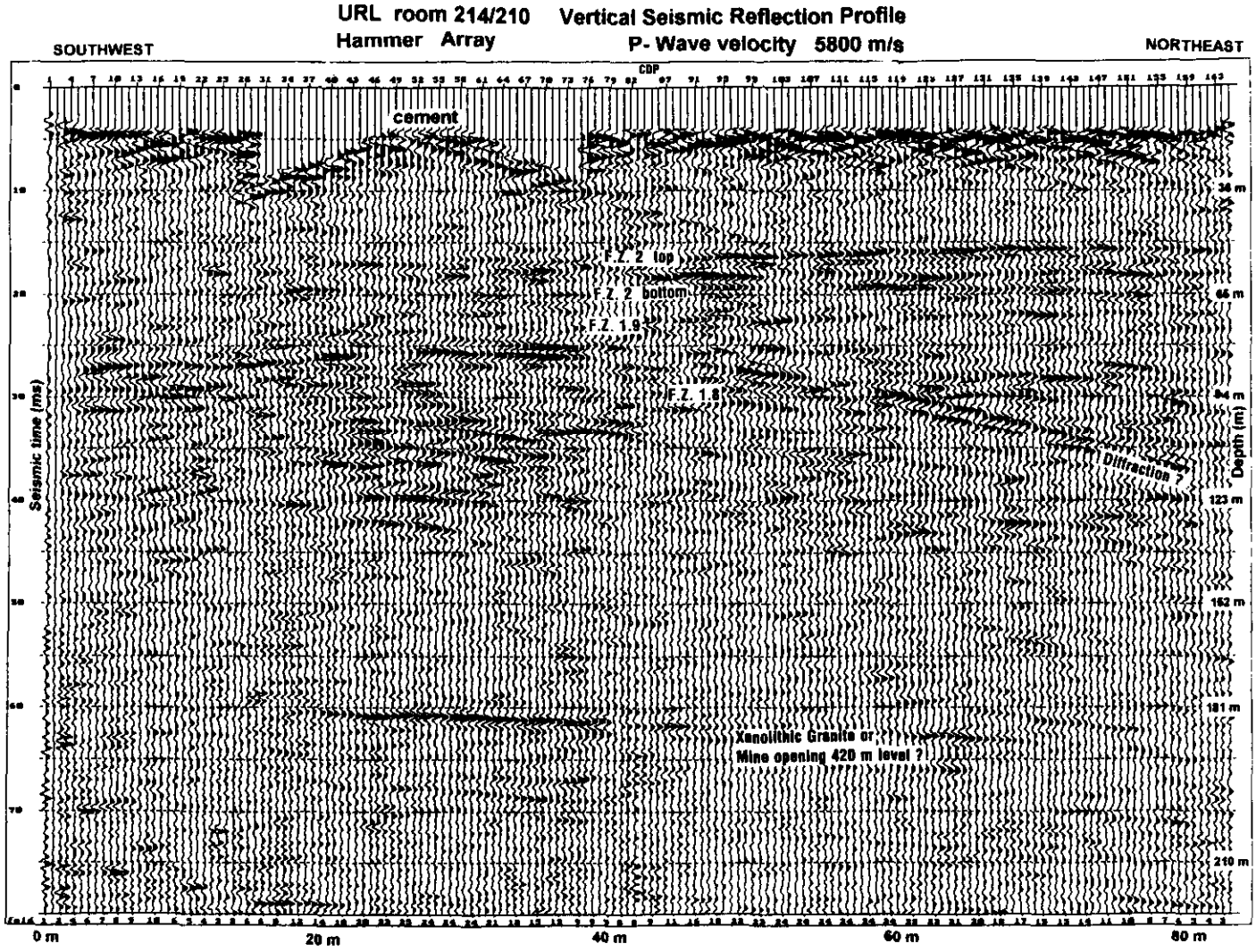


**Fig. 8.** *P*-wave stack (5800 m/s) of hammer source data.

feature could be a diffraction pattern from the shaft. The diffracted wave travelled in a horizontal direction at shear wave speed. Alternatively, the localized mine opening at 300 m is at an appropriate distance to generate the diffracted event observed in the *P*-wave stack section. Unfortunately, the seismic data from only one line are not enough to explain all reflected/diffracted events.

### Shear wave stack

The shear wave stack (Figure 9) shows less energy than the *P*-wave stack but in the interval from 27 ms to 28 ms a distinct reflection appears. This reflection is from the top of FZ-2 but it appears at a later time than the corresponding *P*-wave reflection due to the difference in velocity. Several curving patterns are present in the shear wave stack, one of which corresponds closely to the pattern identified as a shear wave diffraction on the *P*-wave stack (Figure 8). One reflection at 60 ms between 20 m and 40 m chainage is probably *P*-wave energy, the same as shown on Figure 8, not cancelled by the NMO correction. The dominant shear wave frequency is 600 Hz to 700 Hz.

### Explosive source

Figure 10 compares the *P*-wave sections from blasting caps with those from the hammer over a distance of 32 m. The similarity between the two profiles is striking, despite the following differences: hammer data includes a five-blow source array, 24 fold, split spread; cap data is single shot, 12

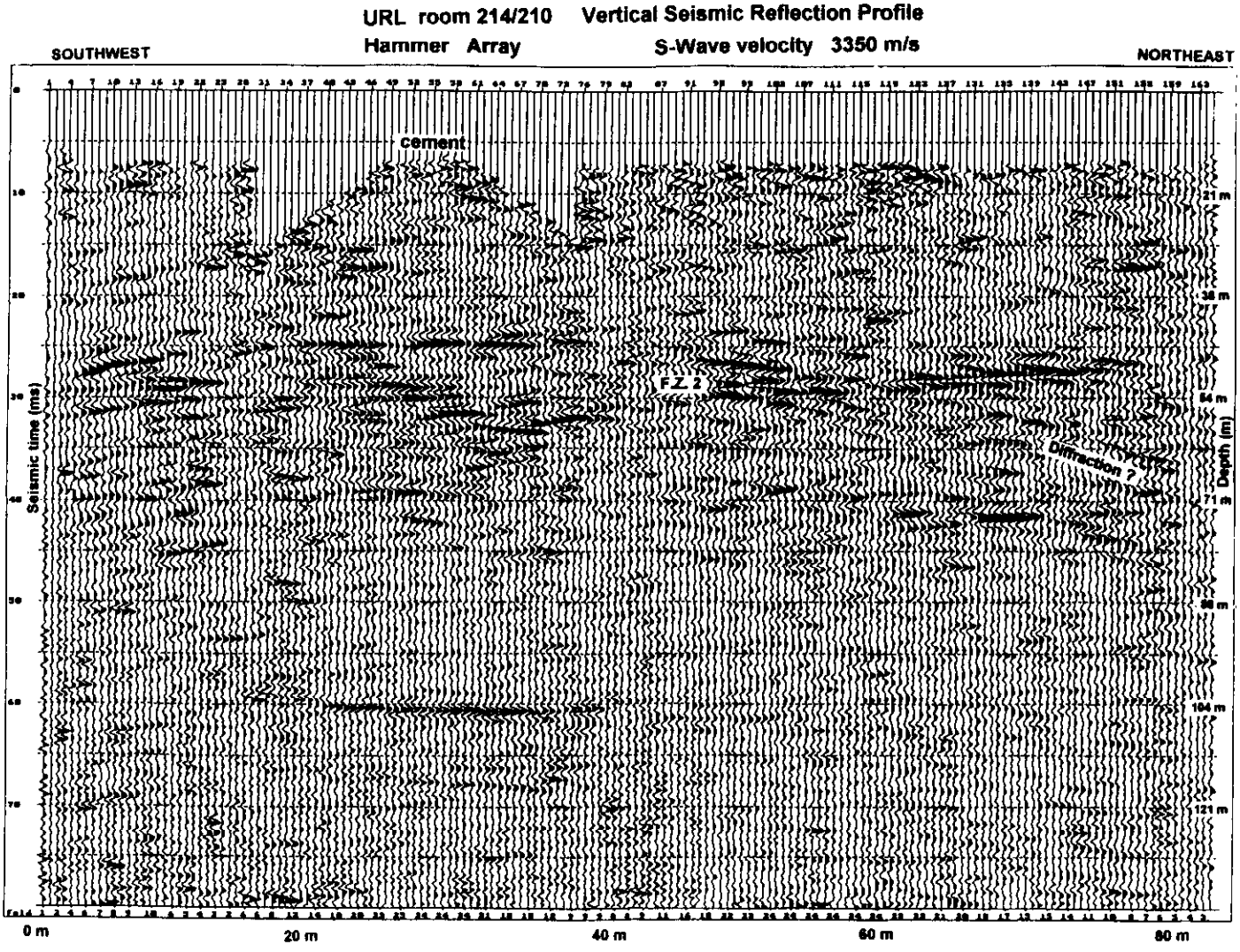


**Fig. 9.** *S*-wave stack (3350 m/s) of hammer source data. Below 40 ms there is little or no differentiation between *P*-wave and *S*-wave types on the basis of stacking velocity for the data shown.

fold, single ended. The noise structure is somewhat different but the principal reflections in each data set are the same, giving confidence in the interpretation despite the high noise level of the original field records.

The cap data were also processed using the shear wave stacking velocity (not shown). The shear wave stack with caps shows reflections similar to the shear wave stack with hammer but with more noise. Both the hammer and the caps seem to produce both *P*-waves and *S*-waves.

## Comparison with radar sounding

Holloway (1992) reported results of radar sounding with 190 MHz equipment in rooms 205 and 207 of the 240 level at URL. Good reflections were obtained from FZ-2 (depth 12 m under room 207) and associated splays at depths to 50 m. Room 207 is parallel and about 80 m updip from room 210 so it is interesting to compare the results even though the reflector depths are different. Resolution of these two methods depends on their respective wavelengths in granite, about 5 m for seismic and about 0.6 m for radar. The radar data are superimposed on the seismic data in Figure 11 with the same depth scales but shifting the radar data down to match the deeper (50 m) fracture zone under room 210. Figure 11 shows that the radar reflections and seismic reflections agree when the difference in depth between room 207 and room 210 is taken into account. Even though the radar wavelength

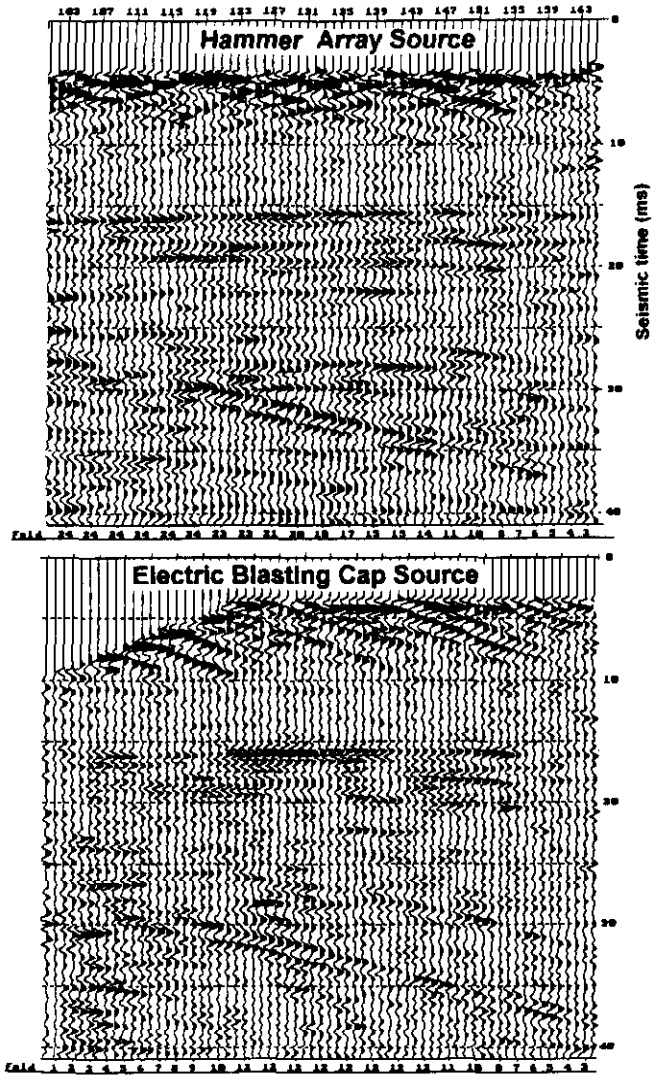


**Fig. 10.** Comparison of *P*-wave stack sections from hammer source and blasting cap sources.

is shorter, each of the radar features has a corresponding seismic expression. The normal depth of penetration for radar is about 30 m, and under ideal conditions, up to 50 m (Holloway, 1992). The seismic data shows clear reflections to depths of 180 m and more. However, the seismic data is limited in resolution of very shallow reflections due to interference from surface waves. The shallowest reflections recognized are from 50 m depth but it appears that seismic reflections as shallow as 30 m depth (15 ms) could be identified if they existed.

## Discussion

These tests demonstrate that high-resolution seismic reflection surveys in underground excavations can detect fracture zones in granite. FZ-2, 50 m below the 240 m level, was detected as a band of reflectors, showing the top and bottom of the zone, and some interior detail. Shear wave reflections were also obtained from FZ-2. Some deeper, thinner fractures and some features of uncertain nature also produced reflections. A diffraction pattern from the shaft or an excavation at the 300-m level was observed. Some of the reflections were confirmed with synthetic seismograms calculated from sonic and density logs of a deep borehole. The high frequency of the seismic waves permits detailed interpretation of the fracture zone.

Similar results with both hammer and cap sources give confidence in the method despite low signal-to-noise ratios on the original field data. The hammer source provides slightly better signal levels, probably because it was used in an array geometry whereas the caps were used singly. The hammer source is preferred because of the ease with which source arrays may be implemented.

The seismic method was able to resolve geological detail in the depth range of 30 m to 200 m and more. Ground-probing radar surveys have produced reflections from fractures and fracture zones in the depth range of 5 to 50 m in this granite. The seismic method has greater depth of penetration than radar. However, for a shallow depth of investigation, the radar method is faster and more convenient than seismic and should have better resolution. In situations where the pore water in the rock is more saline than in these surveys, the radar method may have limited depth penetration. In these cases, the high-resolution seismic method will still provide effective fracture mapping capabilities beyond 30 m.

Good coupling of geophones to the rock is an essential key to success with the high-frequency seismic reflection method. Good coupling of the energy source is equally important and the survey must be designed to record high-frequency signals without aliasing. Surface conditions are important as shown by the loss of data quality where the floor was covered with concrete. Similar quality problems could occur should there be loose slabs of granite under the geophone positions.

## References

Anstey, N.A., 1986, Whatever happened to ground roll?: The Leading Edge **5**, 3, 40-45.

Brown, A., Soonawala, N.M., Everitt, R. and Kamineni, D.C., 1989, Geology and geophysics of the Underground Research Laboratory site, Lac du Bonnet Batholith, Manitoba: Can. J. Earth Sci. **26**, 404-425.

Everitt, R.A. and Reed, R.S., 1990, Geology of the 240 m level of the Underground Research Laboratory: Atomic Energy of Canada Ltd., Technical Report, TR-491-3.

Gendzwill, D.J. and Brehm, R., 1993, High resolution seismic reflections in a potash mine: Geophysics **58**, 741-748.

Holloway, A.L., 1992, Fracture mapping in granite rock using ground probing radar: Geol. Surv. Can., Paper 90-4, 85-100.

Kim, J.S., Moon, W.M., Lodha, G., Serzu, M. and Soonawala, N., 1994, Imaging of reflection seismic energy for mapping shallow fracture zones in crystalline rocks: Geophysics **59**, 753-774.

Martin, C.D., 1990, Characterizing *in situ* stress domains at AECL's Underground Research Laboratory: Can. Geotech. J. **27**, 631-646.

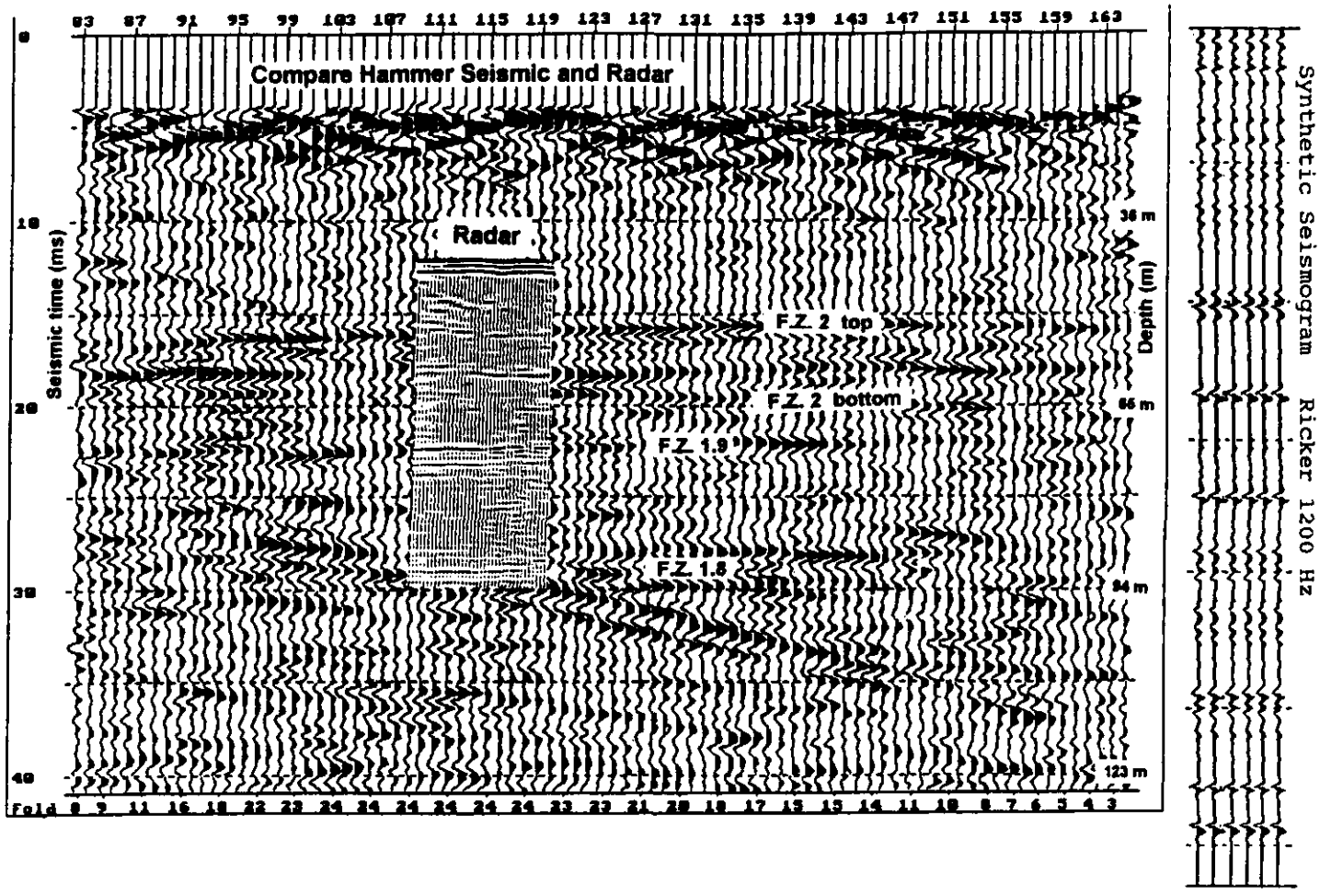


**Fig. 11.** Comparison of radar profile in room 207 with seismic reflections in room 210. Radar depth scale is the same as seismic depth scale but radar data are shifted down to compensate for difference in depth to Fracture Zone 2 between rooms 207 and 210. 1200-Hz synthetic seismogram with AGC (Figure 3) from borehole URL6 is shown for comparison.